Published in final edited form as:
J Biomed Mater Res A. 2010 September 1; 94(3): 870–876. doi:10.1002/jbm.a.32765.

Three-dimensional Macroscopic Scaffolds With a Gradient in Stiffness for Functional Regeneration of Interfacial Tissues

Milind Singh[1], **Nathan Dormer**[2], **Jean R. Salash**[3], **Jordan M. Christian**[3], **David S. Moore**[4], **Cory Berkland**[3,5], and **Michael S. Detamore**[3,*]

[1]Department of Bioengineering, Rice University, Houston, Texas 77005

[2]Bioengineering Program, University of Kansas, Lawrence, Kansas 66045

[3]Department of Chemical and Petroleum Engineering, University of Kansas, Lawrence, Kansas 66045

[4]KU Microscopy and Analytical Imaging Laboratory, University of Kansas, Lawrence, Kansas 66045

[5]Department of Pharmaceutical Chemistry, University of Kansas, Lawrence, Kansas 66045

Abstract

A novel approach has been demonstrated to construct biocompatible, macroporous 3-D tissue engineering scaffolds containing a continuous macroscopic gradient in composition that yields a stiffness gradient along the axis of the scaffold. Polymeric microspheres, made of poly(D,L-lactic-*co*-glycolic acid) (PLGA), and composite microspheres encapsulating a higher stiffness nano-phase material (PLGA encapsulating $CaCO_3$ or TiO_2 nanoparticles) were used for the construction of microsphere-based scaffolds. Using controlled infusion of polymeric and composite microspheres, gradient scaffolds displaying an anisotropic macroscopic distribution of $CaCO_3$/TiO_2 were fabricated via an ethanol sintering technique. The controllable mechanical characteristics and biocompatible nature of these scaffolds warrants further investigation for interfacial tissue engineering applications.

Keywords

Gradient; Interfacial tissue; Tissue engineering; Composite materials; Stiffness

Introduction

Continuous transitional gradients in cellular-extracellular architecture exist throughout the human body, within tissues and at tissue interfaces, to satisfy spatially diverse functional needs.1–2 Interfacial tissue engineering, an emerging field that focuses on regenerating interfaces between the tissues (e.g., bone-cartilage, muscle-tendon, etc.), is a strategic approach to create functional tissue interfaces that 1) may resolve the issues of graft failure at the interface, and 2) may be able to provide mutually inductive endogenous signals from the adjacent tissues that are involved during tissue formation *in vivo*.2 In certain cases, interfacial tissue engineering may also provide an alternative to tissue adhesives,3–4 where

*Corresponding Author, Dr. Michael S. Detamore, Ph.D., Associate Professor, Department of Chemical and Petroleum Engineering, Learned Hall, Room 4132, 1530 W. 15th St., Lawrence, KS 66045 (USA), Phone: (785)-864-4943, Fax: (785)-864-4967, detamore@ku.edu.

There are no conflicts of interest.

bridging a tissue-engineered prosthetic/biomaterial to a native tissue could be achieved by successful integration of one (or both) end(s) of the tissue-engineered substrate directly with the native tissue to facilitate regeneration. Approaches to engineer tissue interfaces, to date, have largely focused on creating graded-structures (e.g., biphasic, triphasic) in cellular/biomaterial composition, which do not closely mimic the continuous transitions of native tissues, a design limitation that may lead to stress concentrations at each interface and eventual failure of the implant.[1–2]

Delivery of genes or growth factors in a continuous gradient manner across a tissue engineering scaffold via biomaterials is a relatively new avenue of research to engineer heterogeneous tissue substrates, where gradation in material properties may be achieved via matrix deposition *in vitro* or *in vivo*.1 An alternative approach could be to utilize a three-dimensional scaffold that contains a continuous gradient in mechanical properties from the beginning, as a functional substrate or a functional implant. Various approaches used to create continuous gradient scaffolds at macro- and micro-scales include diffusion-based or controlled photopolymerization processes, where gradients are generated by altering the cross-linker concentration via diffusion or by controlled photo-exposure (using a gradient photomask or by varying photo-exposure time).[5–9] A major limitation is that these approaches are primarily restricted to the construction of 2-D gel-based substrates. Here, we demonstrate a novel approach to construct biocompatible, macroporous 3-D tissue engineering scaffolds containing a continuous gradient in stiffness. Using polymeric microspheres, made of poly(D,L-lactic-*co*-glycolic acid) (PLGA), and composite microspheres encapsulating a higher stiffness nano-phase material (PLGA encapsulating $CaCO_3$ or TiO_2 nanoparticles), microsphere-based homogeneous and gradient scaffolds were constructed. The controllable mechanical characteristics and biocompatible nature of these scaffolds make them an attractive alternative for a variety of interfacial tissue engineering applications.

Materials and Methods

Materials

PLGA (50:50) (inherent viscosity: 0.36 dL/g) was purchased from Lakeshore Biomaterials. $CaCO_3$ nanoparticles (SOCAL® 31, mean particle size 70 nm) were generously donated by Solvay Chemicals. TiO_2 nanoparticles (<100 nm (Brunauer–Emmett–Teller method)) were purchased from Sigma. Poly(vinyl alcohol) (PVA; 88% hydrolyzed, 25,000 Da) was obtained from Polysciences, Inc. Rhodamine B was purchased from MP Biomedicals, Inc. All cell culture media were supplied by Invitrogen, unless otherwise stated. Dichloromethane (DCM; high pressure liquid chromatography grade) was obtained from Fisher Scientific (Pittsburgh, PA). Ethanol (Absolute - 200 Proof) was obtained in house.

Preparation of microspheres

Uniform microspheres were prepared using technology from our previous reports.[10–12] Briefly, PLGA dissolved in DCM (20% w/v) was sprayed through a small-gauge needle. Using acoustic excitation produced by an ultrasonic transducer, regular jet instabilities were created in the polymer stream that produced uniform polymer droplets. An annular carrier non-solvent stream (0.5% PVA w/v in distilled water (ddH_2O)) surrounding the droplets was produced using a nozzle coaxial to the needle. The emanated polymer/carrier streams flowed into a beaker containing the non-solvent. Incipient polymer droplets were stirred for 3–4 h to allow solvent evaporation, which were then filtered and rinsed with ddH_2O to remove residual PVA. Finally, microspheres were lyophilized for ca. 2 days and stored at −20°C under desiccant. Composite microspheres were prepared likewise, where the polymer stream was replaced with a composite stream that also contained a nano-phase material ($CaCO_3$ or

TiO_2) suspended in the PLGA/DCM solution (sonicated at 50% amplitude for 1 min; in different proportions, % by weight). In a similar manner, fluorescent dye–loaded microspheres were prepared by using a PLGA solution (~20% w/v in DCM) codissolved with rhodamine B.

Preparation of scaffolds

Gradient scaffolds were prepared in a manner described earlier.11 Briefly, two sets of lyophilized microspheres (rhodamine B-loaded PLGA microspheres and 90:10 PLGA:$CaCO_3$ microspheres) were dispersed in ddH_2O at 2.5 % w/v, and separately loaded into two syringes. The suspensions were pumped into a cylindrical glass mold (6 mm diameter, ~ 100 mm height) in a controlled manner using programmable syringe pumps (PHD 22/2000, Harvard Apparatus, Inc.). Using an additional infusion syringe pump and a vacuum pump, a constant level of distilled water was maintained in the mold. Using a filter (particle retention > 3μm) at the bottom of the mold, ddH_2O passed through, while the microparticles stacked in the mold. The stacked microspheres were then sintered using an ethanol treatment (100%) for 2 h.11 The molds (containing the scaffolds) were freeze-dried for a ca. 2 days, and then the scaffolds were retrieved from the molds. Using different preparations of microspheres, various homogeneous scaffolds (containing only one type of microsphere) were prepared in a similar manner. The sets of homogenous scaffolds thus produced included scaffolds made of $CaCO_3$-loaded microspheres (PLGA:$CaCO_3$ at mass ratios of 70:30, 80:20, 90:10, 95:5, 100:0), and TiO_2-loaded microspheres (PLGA:TiO_2 at a mass ratio of 90:10).

Characterization of microspheres and scaffolds

The sizes of the different types of microspheres were determined using a Coulter Multisizer 3 (Beckman Coulter Inc., Fullerton, CA) equipped with a 560-μm aperture. Scanning electron microscopy/ Energy dispersive spectroscopy (SEM/EDS) analysis was performed on intact and cryofractured microspheres using a LEO 1550 field emission scanning electron microscope equipped with an energy dispersive system with a SiLi detector (EDAX, Mahwah, NJ) at 20 kV accelerating voltage, and pixel maps were formed using EDAX genesis software package. Scaffolds prepared using dye-loaded microspheres were imaged under UV light using a UV lamp (254/365 nm; UVGL-25, UVP, Inc., Upland, CA) and a high-resolution camera, and images were analyzed using NIH ImageJ software to assess spatial distribution of the dye molecules.

Mechanical testing

Mechanical characterization of the scaffolds was performed under uniaxial, unconfined compression (Instron Model 5848, Canton, MA; 50 N load cell). The average dimension of the samples and sample size (n) are indicated in Table 1. Samples were tare-loaded (0.1 N, i.e., ~3.5 kPa), then compressed at a strain rate of 1% s^{-1} under phosphate buffered saline (0.138 M NaCl, 0.0027 M KCl) at 37 °C. Moduli of elasticity were obtained from the initial linear regions of the stress-strain curves at either 25% strain or the onset of the non-linear region (rationale explained later).11,13

Cell Culture and seeding

For the cell culture studies, human umbilical cord mesenhymal stromal cells (hUCMSCs) were selected, as these cells have recently shown potential for musculoskeletal tissue repair.14–16 Cells were harvested from one human umbilical cord obtained from the University of Kansas Medical Center (KU Medical Center IRB approval no. 10951, KU-Lawrence IRB approval no. 15402; informed signed consent was obtained prior to the delivery) as described earlier.17 The cell culture medium consisted of low glucose Dulbecco's Modified

Eagle's Medium (DMEM-LG), 10% FBS (Gemini), and 1% penicillin streptomycin (PS). Cells (expanded to passage 4, suspended in 75 μL medium) were seeded onto scaffolds (90:10 mass ratio of PLGA:$CaCO_3$; sterilized using ethylene oxide) drop-wise at a density of 10×10^6 cells mL^{-1} in a 24 well untreated plate, then 1 mL of culture medium was added into wells.

Viability assessment

Cells were cultured for 2 weeks onto scaffolds, with half of the media changed every other day. Subsequently, cell viability was evaluated by staining the scaffolds using a LIVE/DEAD reagent (2 μM calcein AM, 4 μM ethidium homodimer-1; Molecular Probes) followed by a 45 min incubation at room temperature, before being subjected to fluorescence microscopy (Olympus/Intelligent Innovations Spinning Disk Confocal Microscope).

Statistics

Moduli values obtained at either 25% strain or the onset of the non-linear region were compared using a six-level single factor analysis of variance (ANOVA), followed by a Tukey's Honestly Significant Difference *post hoc* test when significance was detected.

Results

Microspheres were characterized for their size and morphology (Fig. 1). Coulter Multisizer size distribution plots demonstrated the high monodispersity of microspheres, with their average diameters each in the range of 130–175 μm following solvent extraction (Fig. 1A). Morphological assessment of intact and cryofractured microspheres with scanning electron microscopy (SEM) indicated that encapsulation of nano-phase materials led to changes in the typically smooth surface and interior morphology of PLGA microspheres (Fig. 1B, D compared to F). In general, encapsulation of nano-phase $CaCO_3$ resulted in the formation of submicron-sized pores throughout the microspheres, possibly indicating that a portion of the $CaCO_3$ leached out of the microspheres during solvent evaporation (Fig. 1B). In contrast, TiO_2-encapsulated microspheres displayed a smooth exterior and less porous interior (Fig. 1D). SEM/EDS was performed to determine the distribution of nano-phase materials within the microspheres qualitatively. The presence of Ca and Ti were each confirmed via EDS. The elemental distribution of Ca and Ti, as observed via SEM/EDS on the surface and interiors of the microspheres, confirmed the presence of $CaCO_3$ and TiO_2 in respective composite microspheres (Fig. 1C, E), where agglomeration of nano-phase materials at several locations was evident.

Microsphere-based scaffolds were prepared using an ethanol sintering method, where ethanol was used as an agent to sinter the adjoining microspheres.11 Homogeneous cylindrical scaffolds, prepared using a 2 h duration of ethanol soaking, were characterized for their morphology and cytotoxicity (Fig. 2). Scanning electron micrographs of a representative scaffold, prepared by sintering the composite microspheres (90:10 PLGA:$CaCO_3$), displayed the typical porous nature of the scaffold and microsphere fusion sites (Fig. 2B–C). The compatibility of scaffolds with human umbilical cord mesenchymal stromal cells (hUCMSCs) was also assessed. For this study, cells were seeded on the scaffolds (90:10 PLGA:$CaCO_3$) drop-wise, and statically cultured for 2 wks. HUCMSCs inside the scaffolds were imaged by fluorescence imaging of a fractured scaffold using a Live/Dead assay, which demonstrated high cell viability (green fluorescence) (Fig. 2D).

Gradient scaffolds containing an anisotropic distribution of $CaCO_3/TiO_2$ were prepared to demonstrate a continuous gradient of mechanical stiffness within constructs. Using a

gradient generation methodology described earlier,11 gradient scaffolds were prepared via controlled infusion of two separately-loaded microsphere suspensions (in ddH_2O) into a cylindrical glass mold using two programmable syringe pumps followed by an ethanol sintering for 2 h. The pumps were co-programmed to provide a linearly increasing flow profile for one microsphere suspension and a linearly decreasing profile for the other suspension, thus, maintaining a constant overall flow rate. To visualize the gradient, a scaffold was created using dye (Rhodamine B)-loaded PLGA microspheres and composite (90:10 PLGA:$CaCO_3$) microspheres, which were flowed into the mold then fused using a 2 h ethanol soak (Fig. 3). Two-dimensional image analysis revealed that the fluorescence intensity of white pixels increased in a continuous gradient across the length of the scaffold, indicating an increase in the ratio of composite to dye-loaded microspheres along the axis of the scaffold (Fig. 3A). To determine the effect of the inclusion of nano-phase materials on the overall properties of the scaffolds, homogeneous scaffolds constructed using different microsphere types were subjected to uniaxial unconfined compression testing. Compression of microsphere-based scaffolds under hydrated conditions results in a typical stress-strain curve, where an initial linear region, representing the matrix stiffness, is followed by a non-linear pore-collapse regime and a material densification regime, respectively.11 Pore-collapse for the composite scaffolds usually began at ~40% strain compared to ~25% strain corresponding to the control PLGA scaffolds. The moduli of elasticity evaluated at a fixed strain value (25% strain) and preceding the onset of pore-collapse (40% for the composite microspheres and 25% for the control microspheres) are reported (Fig. 3B). The average maximum matrix stiffness, corresponding to the onset of the pore-collapse regime, was found to be higher for the scaffolds prepared using composite microspheres having a higher $CaCO_3$ content (20% and 30% by wt) compared to the controls. Scaffolds prepared using 90:10 PLGA:$CaCO_3$ (percent by wt) demonstrated a lower matrix stiffness, in general. The aforementioned differences, however, were found not to be statistically significant. Compared to control PLGA scaffolds, scaffolds prepared using 95:5 PLGA:$CaCO_3$ also demonstrated a lower matrix stiffness. The difference in moduli measured at 25% strain was found to be statistically significant ($p < 0.05$).

Discussion

Various methods to fabricate microsphere-based scaffolds have been investigated in the past, including heat-sintering,18⁻19 a solvent vapor treatment (dichloromethane),20⁻21 a solvent/non-solvent sintering method (acetone and ethanol treatment),22⁻23 or a non-solvent sintering technique (ethanol treatment).11 The primary impetus to use microspheres as the building blocks of a scaffold is the versatility that the microspheres provide in controlling the release kinetics of encapsulated factors. Moreover, heterogeneous arrangement of two different types of microspheres along the axis of the scaffold may allow macroscopic spatial control over the scaffold morphology or spatiotemporal control over the delivery of encapsulated factors. In this regard, microsphere size is a major determinant of polymer degradation rate, and is a primary factor governing the release kinetics of loaded molecules.24 In the present study, PLGA/composite microspheres were prepared via an emulsion/solvent extraction method using technology from our previous reports, resulting in a relatively monodisperse microsphere size distribution compared to traditional microsphere fabrication techniques.11⁻12 Composite suspensions were prepared by dispersing nano-phase materials in a PLGA solution (dissolved in dichloromethane (DCM)) in different proportions. Controlled regular jet instabilities created by an ultrasonic transducer resulted in cleaving the polymer/composite stream into uniform droplets that hardened into microspheres following solvent extraction.11 The microspheres thus produced were highly monodisperse (Fig. 1).

To translate the use of microsphere-based scaffolds for interfacial tissue engineering, this study investigated a method to create gradient scaffolds that exhibited a continuous gradient in the composition. Using polymeric microspheres, made of poly($_{D,L}$-lactic-*co*-glycolic acid) (PLGA), and composite microspheres encapsulating a higher stiffness nano-phase material (PLGA encapsulating $CaCO_3$ or TiO_2 nanoparticles), microsphere-based homogeneous and gradient scaffolds were constructed. An ethanol sintering method was used to prepare the scaffolds,11 where reptation of the polymeric chains at the site of contact was hypothesized to lead to the sintering of the adjoining microspheres. In our previous study, the duration of ethanol sintering was found to be an important process parameter affecting the extent of sintering of PLGA microspheres, where a 1 – 2 h ethanol soak resulted in higher average elastic moduli of the resulting scaffolds compared to a 30 min ethanol soak (around 300 KPa and 150 KPa, respectively).11 In the present study, the average stiffness of the PLGA scaffolds (control group) prepared using a 2 h ethanol soak was found to be consistent with the previous observation (~300 KPa). Our previous study, however, differed from the current study in the intrinsic viscosity of the PLGA used (0.36 dL/g vs 0.41 dL/g, respectively). In addition, a proof-of-concept was developed using dye-loaded and blank microspheres for evaluation of the gradient in composition. As the adapted method ascertained limited accuracy due to the semi-quantitative nature of analysis, more accurate quantitative assessment of gradient profiles generated in composition as well as stiffness warrants development of direct measurement techniques.

A limitation of the approach was that mechanical stiffness gradients were not directly measured. Rather, the gradients in stiffness were demonstrated by creating scaffolds of nanocomposite microspheres, which were shown to change the macroscopic stiffness in homogeneous constructs, and then creating scaffolds with a gradual transition from microspheres of one material on one side to microspheres of another material on the other side. Although additional analyses with their own inherent limitations could have been implemented—such as microindentation of points along the surface, dividing extended-length gradient scaffolds into sections and testing those sections, or marking points along the surface and recording strains under compression by video—their is significance associated with the approach and findings of this study in that it was the first to demonstrate that materials of different stiffness could be continuously transitioned from one side of a scaffold to another using nanocomposite microspheres.

In vitro cell culture studies demonstrated the feasibility of utilizing these matrices for *in vitro* tissue engineering. The cell viability observed in the representative homogeneous composite scaffolds provided preliminary evidence for the suitability of these scaffolds for *in vitro* tissue engineering. However, future efforts will be needed to perform a comprehensive quantitative evaluation of cell survival and matrix synthesis as a function of type, size and encapsulated content of nano-phase material.

In the present study, although the inclusion of nano-phase materials in the microspheres was expected to lead to an increase in stiffness of the microspheres, the overall average stiffness of the composite scaffolds was found to be lower compared to control PLGA scaffolds at a fixed strain value (25% strain) (Fig. 3). This suggested that the presence of the nano-phase materials interfered with the ethanol sintering process, resulting in a lower extent of sintering of composite microspheres for a 2 h ethanol-soak, and likely a higher porosity, compared to the control PLGA microspheres. It is possible that the surface modifications resulting from the incorporation of nano-phase materials led to a decrease in the extent of sintering of the composite microspheres by adversely affecting the polymer reptation near the contact sites, thus yielding a lower stiffness of the scaffolds. Scaffold morphology as observed by SEM substantiated this hypothesis, where a decreased extent of sintering was visualized for scaffolds made of 90:10 PLGA:$CaCO_3$ microspheres compared to control

PLGA scaffolds (compare Fig. 2 A vs. B). For composite microspheres, increasing the relative content of $CaCO_3$, however, led to an increase in the average scaffold stiffness. In addition, scaffolds constructed using TiO_2-encapsulated microspheres displayed a higher average stiffness compared to scaffolds with $CaCO_3$-encapsulated microspheres. Moreover, inclusion of a nano-phase material ($CaCO_3$ or TiO_2 at 10 % (wt/wt) or higher) and subsequent ethanol sintering for 2 h resulted in a higher average stiffness of the scaffold (in the range of 150 – 400 KPa), compared to a 30 min ethanol soak of PLGA microspheres in a previous study, which appeared to have a similar degree of sintering.11 These results are suggestive that the extent of sintering (e.g., duration of ethanol exposure) is an important factor, possibly more dominating than the composition of the microspheres under certain conditions, for the overall integrity of the scaffold, and both can be selectively altered to tailor the mechanical properties of the scaffold. Future studies will be conducted to investigate the effect of the extent of sintering at a given composition of nano-phase material to PLGA as well as evaluation of other nanophase materials such as hydroxyapatite.

Conclusion

Using composite microspheres (containing nano-phase $CaCO_3/TiO_2$) and polymeric microspheres, a method to prepare scaffolds containing a gradient distribution in the nano-phase material was demonstrated. The extent of sintering, composition of the microspheres and the relative content of the two microsphere types can be selectively varied to alter the stiffness of the matrix to create regular and inverse-gradients in mechanical properties. The approach described here presents biocompatible and porous macroscopic 3-D scaffolds with controllable mechanical propertie s for tissue engineering, and gradient scaffolds that may be particularly useful for interfacial tissue regeneration. Integration of controlled release strategies (e.g., growth factors) via microspheres would be straightforward and can be extended to the fabrication of acellular implantable devices for translational tissue regeneration applications.

Acknowledgments

The present work was supported by NIH/NIDCR grant 1 R21 DE017673-01A1 (MSD), the Juvenile Diabetes Research Foundation (CB) and the University of Kansas General Research Fund. We gratefully acknowledge Professor Stevin Gehrke for insightful comments pertaining to the study.

References

1. Phillips JE, Burns KL, Le Doux JM, Guldberg RE, Garcia AJ. Engineering graded tissue interfaces. Proc Natl Acad Sci U S A. 2008; 105(34):12170–12175. [PubMed: 18719120]
2. Singh M, Berkland C, Detamore MS. Strategies and Applications for Incorporating Physical and Chemical Signal Gradients in Tissue Engineering. Tissue Eng Part B Rev. 2008; 14(4):341–366. [PubMed: 18803499]
3. Mahdavi A, Ferreira L, Sundback C, Nichol JW, Chan EP, Carter DJ, Bettinger CJ, Patanavanich S, Chignozha L, Ben-Joseph E, et al. A biodegradable and biocompatible gecko-inspired tissue adhesive. Proc Natl Acad Sci U S A. 2008; 105(7):2307–2312. [PubMed: 18287082]
4. Wang DA, Varghese S, Sharma B, Strehin I, Fermanian S, Gorham J, Fairbrother DH, Cascio B, Elisseeff JH. Multifunctional chondroitin sulphate for cartilage tissue-biomaterial integration. Nat Mater. 2007; 6(5):385–392. [PubMed: 17435762]
5. Wong JY, Velasco A, Rajagopalan P, Pham Q. Directed movement of vascular smooth muscle cells on gradient-compliant hydrogels. Langmuir. 2003; 19(5):1908–1913.
6. Jacot JG, Dianis S, Schnall J, Wong JY. A simple microindentation technique for mapping the microscale compliance of soft hydrated materials and tissues. J Biomed Mater Res A. 2006; 79(3): 485–494. [PubMed: 16779854]

7. Lin-Gibson S, Landis FA, Drzal PL. Combinatorial investigation of the structure-properties characterization of photopolymerized dimethacrylate networks. Biomaterials. 2006; 27(9):1711–1717. [PubMed: 16310845]
8. Zaari N, Rajagopalan P, Kim SK, Engler AJ, Wong JY. Photopolymerization in Microfluidic Gradient Generators: Microscale Control of Substrate Compliance to Manipulate Cell Response. Adv Mater. 2004; 16(23–24):2133–2137.
9. Engler AJ, Richert L, Wong JY, Picart C, Discher DE. Surface probe measurements of the elasticity of sectioned tissue, thin gels and polyelectrolyte multilayer films: Correlations between substrate stiffness and cell adhesion. Surf Sci. 2004; 570(1–2):142–154.
10. Singh M, Sandhu B, Scurto A, Berkland C, Detamore MS. Microsphere-based scaffolds for cartilage tissue engineering: Using subcritical CO(2) as a sintering agent. Acta Biomater. 2009 doi:10.1016/j.actbio.2009.07.042.
11. Singh M, Morris CP, Ellis RJ, Detamore MS, Berkland C. Microsphere-Based Seamless Scaffolds Containing Macroscopic Gradients of Encapsulated Factors for Tissue Engineering. Tissue Eng Part C Methods. 2008; 14(4):299–309. [PubMed: 18795865]
12. Berkland C, Kim K, Pack DW. Fabrication of PLG microspheres with precisely controlled and monodisperse size distributions. J Control Release. 2001; 73(1):59–74. [PubMed: 11337060]
13. Gibson, LJ.; Ashby, MF. Cellular Solids: Structure and Properties. Cambridge University Press; 1997.
14. Wang L, Detamore MS. Insulin-like growth factor-I improves chondrogenesis of predifferentiated human umbilical cord mesenchymal stromal cells. J Orthop Res. 2009; 27(8):1109–1115. [PubMed: 19195026]
15. Wang L, Seshareddy K, Weiss ML, Detamore MS. Effect of Initial Seeding Density on Human Umbilical Cord Mesenchymal Stromal Cells for Fibrocartilage Tissue Engineering. Tissue Eng Part A. 2009; 15(5):1009–1017. [PubMed: 18759671]
16. Wang L, Singh M, Bonewald LF, Detamore MS. Signalling strategies for osteogenic differentiation of human umbilical cord mesenchymal stromal cells for 3D bone tissue engineering. J Tissue Eng Regen Med. 2009; 3(5):398–404. [PubMed: 19434662]
17. Wang L, Seshareddy K, Weiss ML, Detamore MS. Effect of Initial Seeding Density on Human Umbilical Cord Mesenchymal Stromal Cells for Fibrocartilage Tissue Engineering. Tissue Eng Part A. 2008
18. Borden M, Attawia M, Khan Y, El-Amin SF, Laurencin CT. Tissue-engineered bone formation in vivo using a novel sintered polymeric microsphere matrix. J Bone Joint Surg Br. 2004; 86(8): 1200–1208. [PubMed: 15568538]
19. Yao J, Radin S, Leboy PS, Ducheyne P. The effect of bioactive glass content on synthesis and bioactivity of composite poly (lactic-co-glycolic acid)/bioactive glass substrate for tissue engineering. Biomaterials. 2005; 26(14):1935–1943. [PubMed: 15576167]
20. Jaklenec A, Hinckfuss A, Bilgen B, Ciombor DM, Aaron R, Mathiowitz E. Sequential release of bioactive IGF-I and TGF-beta(1) from PLGA microsphere-based scaffolds. Biomaterials. 2008; 29(10):1518–1525. [PubMed: 18166223]
21. Jaklenec A, Wan E, Murray ME, Mathiowitz E. Novel scaffolds fabricated from protein-loaded microspheres for tissue engineering. Biomaterials. 2008; 29(2):185–192. [PubMed: 17950842]
22. Brown JL, Nair LS, Laurencin CT. Solvent/non-solvent sintering: a novel route to create porous microsphere scaffolds for tissue regeneration. J Biomed Mater Res B Appl Biomater. 2008; 86B(2):396–406. [PubMed: 18161819]
23. Nukavarapu SP, Kumbar SG, Brown JL, Krogman NR, Weikel AL, Hindenlang MD, Nair LS, Allcock HR, Laurencin CT. Polyphosphazene/Nano-Hydroxyapatite Composite Microsphere Scaffolds for Bone Tissue Engineering. Biomacromolecules. 2008; 9(7):1818–1825. [PubMed: 18517248]
24. Berkland C, Kim K, Pack DW. PLG microsphere size controls drug release rate through several competing factors. Pharm Res. 2003; 20(7):1055–1062. [PubMed: 12880292]

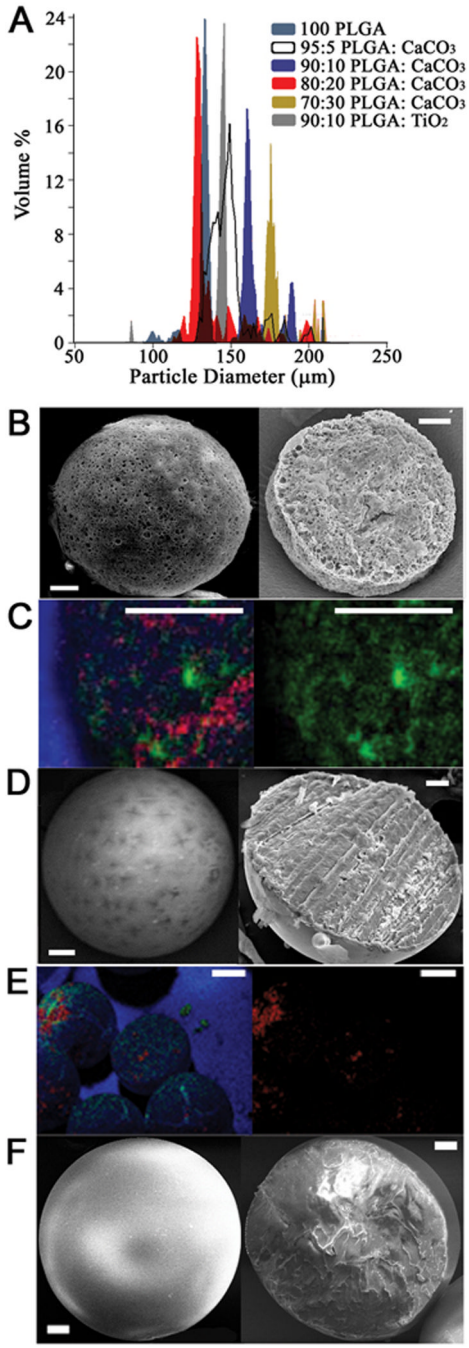

Figure 1.

(A) Coulter multisizer size distribution plot of microspheres of different types (PLGA-$CaCO_3$/TiO_2) prior to lyophilizing, displaying their relative monodispersity and nominal sizes (average diameters: 130–175 μm). Peaks with percent volume less than 0.5% have been omitted for the sake of clarity. (B–F) Morphological analysis of microspheres using scanning electron microscopy/energy dispersive spectroscopy (SEM/EDS). Panels B, D and F display representative SEM images of intact (left) and cryofractured (right) microspheres, corresponding to 90:10 mass ratio PLGA:$CaCO_3$, 90:10 PLGA:TiO_2, and PLGA-only respectively. Panels C and E show the elemental distribution of the microspheres obtained using EDS, displaying an overlay of C, O, and Ca/Ti (left) and corresponding Ca/Ti

distribution (right) (Panel C – cryofractured 90:10 PLGA:$CaCO_3$, color scheme C/O/Ca blue/red/green; Panel E – intact 90:10 PLGA:TiO_2, color scheme C/O/Ti blue/green/red). Scale bars: 20 μm (B–D and F) and 50 μm (E).

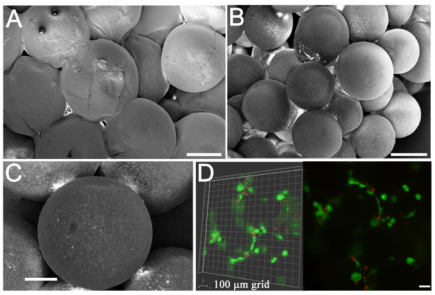

Figure 2.

(A) SEM micrographs of a scaffold prepared by sintering PLGA microspheres using ethanol sintering for 2 h. (B, C) Characteristic SEM micrographs of a scaffold, prepared by sintering the microspheres (90:10 PLGA:$CaCO_3$) using ethanol sintering for 2 h, displaying the porous nature of the scaffold (A) and typical microsphere connection sites (B). Scale bar: 100 and 50 µm for A and B, respectively. (D) Live-dead images of human umbilical cord mesenchymal stromal cells cultured on these scaffolds for a period of 2 weeks, demonstrating high viability (green = live, red = dead). The representative images of cells in a 100 µm thick section (left) and a single plane (right) were taken from an interior section of a scaffold fractured cross-sectionally, where the spatial relationship between the cells and the microspheres (dark regions) can be visualized. Scale bar: 100 µm (C).

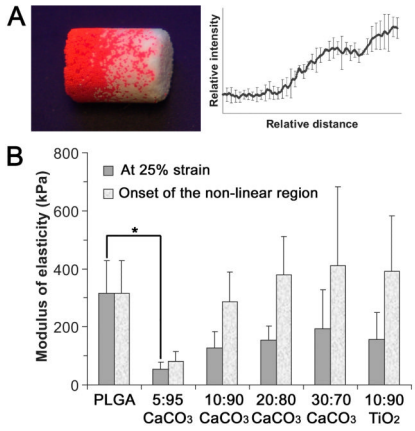

Figure 3.

(A) A proof-of-concept gradient scaffold prepared using dye (Rhodamine B)-loaded PLGA microspheres and 90:10 PLGA:$CaCO_3$ microspheres using a 2 h ethanol soak. The image was taken under UV light using a UV lamp (254/365 nm; UVGL-25, UVP, Inc.) and a high-resolution camera, and analyzed using NIH ImageJ software to plot relative intensity as a function of pixel distance. (n = 5) (B) Moduli of elasticity of the homogeneous scaffolds prepared using different types of microspheres (means and standard deviations, n = 4, except for groups with 5%, 10% and 20% $CaCO_3$ (n = 3)). The moduli were obtained from the initial linear regions of the stress-train curve: 1) at 25% strain (preceding the onset of pore-collapse for PLGA scaffolds), and 2) preceding the onset of pore-collapse, in general (at 40% strain for composite scaffolds). Surface modifications (see Fig. 1) that resulted due to the incorporation of nano-phase materials led to a decrease in the extent of sintering of the composite microspheres compared to the control PLGA microspheres for a 2 h ethanol-soak. * indicates that the difference was statistically significant ($p < 0.05$).

Table 1

The dimensions and sample size of the scaffolds prepared for mechanical characterization[a]

Scaffold groups	Diameter (mm)	Height (mm)	Sample size (n)
PLGA :$CaCO_3$ 100:0	5.6 ± 0.4	3.9 ± 0.7	4
PLGA :$CaCO_3$ 95:5	5.5 ± 0.3	4.2 ± 0.5	3
PLGA :$CaCO_3$ 90:10	5.7 ± 0.2	3.9 ± 0.8	3
PLGA :$CaCO_3$ 80:20	5.6 ± 0.2	3.9 ± 0.2	3
PLGA :$CaCO_3$ 70:30	5.5 ± 0.1	5.4 ± 0.7	4
PLGA :TiO_2 90:10	5.4	4.5 ± 1.1	4

[a]Mean ± S.D.